

## Precision Measurement of the $K$ -Shell Spectrum from Highly Charged Xenon with an Array of X-Ray Calorimeters

Daniel B. Thorn,\* Ming F. Gu, Gregory V. Brown, and Peter Beiersdorfer  
*Lawrence Livermore National Laboratory, Livermore, California 94550, USA*

F. Scott Porter, Caroline A. Kilbourne, and Richard L. Kelley  
*Goddard Space Flight Center, NASA, Maryland 20771, USA*  
(Received 8 December 2008; published 15 October 2009)

We present a measurement of the  $K$ -shell spectrum from highly charged xenon ions recorded with a high-energy x-ray calorimeter spectrometer array that can distinguish between various theories for the atomic structure of the two electron system. The array was designed to provide high resolution with high quantum efficiency in the 10–60 keV x-ray range which allows us to resolve blends that afflicted previous measurements. A precision of better than 2 eV was achieved in the measurement of the  $\text{Xe}^{52+}$  and  $\text{Xe}^{53+}$   $K$ -shell transitions located near 31 keV, which is an order of magnitude better than previously reported.

DOI: 10.1103/PhysRevLett.103.163001

PACS numbers: 32.30.Rj, 29.40.Vj, 31.30.J-, 32.10.Fn

High- $Z$  ions represent a test bed for strong field quantum electrodynamics (QED). Heliumlike ions, in particular, are stepping stones for developing multielectron QED theories. In addition, accurate knowledge of energy levels in heliumlike ions are crucial for proposed atomic parity nonconservation experiments [1–3]. However, theoretical calculations diverge by over an eV for  $\text{Xe}^{52+}$  and by nearly 10 eV at  $\text{U}^{90+}$ . Thus far, measurements have only been able to distinguish, and then guide, theory for the heliumlike system up to  $\text{Kr}^{34+}$  [4], and thus new measurements are needed. The state of the art for measuring  $K$ -shell spectra of highly charged high- $Z$  ions has revolved around high-purity (Ge) solid state detectors. These detectors were employed in the first measurements of the  $K$ -shell spectra of highly charged xenon and uranium ions [5–9], and are still used today for such measurements [10]. In the case of heliumlike ions, the roughly 150–300 eV resolution of solid state detectors precluded resolving, and thus taking into account, line blends between the singlet,  $(1s2p_{3/2})_1 \rightarrow (1s^2)_0$ , and triplet,  $(1s2p_{3/2})_2 \rightarrow (1s^2)_0$ , transitions.

X-ray calorimeters are devices that determine the energy of x-ray photons by measuring the temperature rise in a material as it absorbs the photon [11]. Originally, they were developed for x-ray measurements below 10 keV, and they have been successfully used on rockets [12], in the laboratory [13,14], and in orbit [15] to measure the  $K$ -shell emission from carbon to iron ions. X-ray calorimeters do not yet provide the resolving power afforded by standard crystal spectrometers, and thus they do not compete with the precision achievable, in principle, by crystal spectrometers in this energy range [16]. However, for  $K$ -shell spectroscopy of high- $Z$  ions ( $Z > 36$ ), which are difficult to produce in large quantities, the use of crystal spectrometers has been unworkable due to low throughput so that high-purity Ge (HPGe) detectors have been the only option. X-ray calorimeters are thought to be competitive with

HPGe detectors, as they promise to have a much higher resolving power (an order of magnitude or more), provided arrays can be built with suitable quantum efficiency (QE).

Here we report on the first use of an x-ray calorimeter spectrometer array with sufficiently high QE to perform a highly precise measurement of the energies of the hard x-ray  $K$ -shell transitions in  $\text{Xe}^{52+}$  and  $\text{Xe}^{53+}$  ions. Ultimately, such a device will enable the study of systems as high as hydrogenlike uranium and beyond. Most importantly, the high resolution eliminates the unaccountable systematic errors associated with line blending that has affected measurements in the past.

Early attempts at using x-ray calorimeters for the  $K$ -shell spectroscopy of highly charged high- $Z$  ions have suffered from the intrinsically small size, i.e., the small solid angle subtended, combined with the low photon flux from available ion sources. For example, a measurement using a single bismuth absorber pixel [17] had a resolution of 80 eV at the Pr  $K$ -shell energy of 37 keV, but, given its small size, the measurement was only able to confirm the idea that x-ray calorimeters could in principle make good measurements of high- $Z$  ions. In an effort to increase the QE for high-energy photons, the EBIT calorimeter spectrometer (ECS) [18] detector was developed. It is a hybrid array designed and built to take into account the needs of both low- $Z$  and high- $Z$  spectroscopic needs. The ECS has 32 pixels of which 18 are 8  $\mu\text{m}$  thick HgTe used for low-energy work, and 14 are  $\sim 100$   $\mu\text{m}$  thick HgTe used for the present high-energy x-ray measurements.

The measurements were performed at the Lawrence Livermore National Laboratory's SuperEBIT high-energy electron beam ion trap [19]. Hydrogenlike through boronlike ions were produced and excited by repeated electron collisions with a 114 keV, 200–240 mA electron beam. The ions were trapped in an axial potential of 80 V and a radial potential of about 10 V due to the space charge from the

electron beam. Xenon was injected into the trap via a ballistic gas injector system. Radiation from the trap region was viewed perpendicular to the electron beam direction and had to traverse a 30 cm air gap and two 125  $\mu\text{m}$  beryllium windows to reach the x-ray calorimeter array. The Be windows allowed for an air gap where radioactive sources could be placed. Figure 1 shows the spectrum from 85 h of data taken with the ECS.

EBIT produces a low flux of photons, and taken together with the small size of each detector element, only a few counts in each pixel per day were recorded. To account for possible day-to-day shifts in the energy scale, a strong calibration line was recorded in each pixel on each day. This was achieved by inserting radioactive  $^{133}\text{Ba}$  and  $^{241}\text{Am}$  sources in front of the ECS.  $^{133}\text{Ba}$  decays via electron capture to  $^{133}\text{Cs}$  and produces Cs  $K\alpha$  x rays at roughly 30 keV.  $^{241}\text{Am}$  produces a plethora of  $x$  and  $\gamma$  rays from 10 to 60 keV. The  $^{133}\text{Ba}$  source was inserted in front of the calorimeter at the beginning of each data run for 1 h and then at the end of the run to check for any intraday drifts (no drifts were found). The xenon data runs were typically 10 h long. At the end of a xenon data run and after placing the  $^{133}\text{Ba}$  source in front of the ECS, an  $^{241}\text{Am}$  source was inserted overnight to obtain the calibration of the energy dispersion of the detector. Both a linear and a quadratic fit for the energy scale was produced using lines from the  $^{241}\text{Am}$  and  $^{133}\text{Ba}$  sources. Each gave similar results and the maximum difference in the two was taken as the error in the determination of the calibration curve (0.6 eV). The linear fit to the Ba lines was used as the final energy scale for the experiment.

The power incident on the detector can, in some cases, affect the measured centroid of a line. Indeed, a shift of

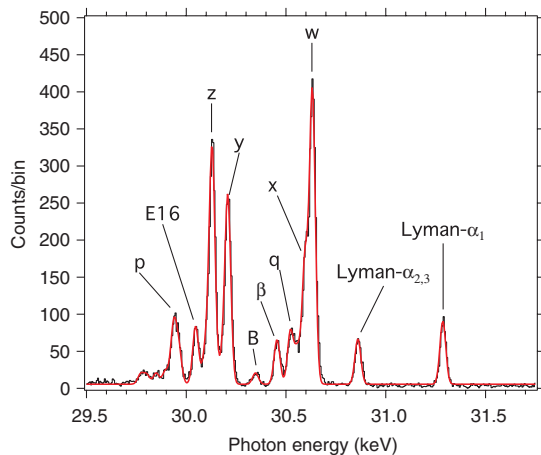


FIG. 1 (color online). X-ray calorimeter spectrum of hydrogenlike through boronlike xenon taken at an electron beam energy of 114 keV. The hydrogenlike lines are labeled as Lyman- $\alpha_{1-3}$ ; the heliumlike and lithiumlike lines  $w$ ,  $q$ ,  $y$ , and  $z$  are labeled according to [29]; the berylliumlike lines  $\beta$  and E16 are labeled according to [30] and [31], respectively; the boronlike line is labeled as  $B$ .

the centroids of the lines measured under high-power (calibration) versus low-power (xenon  $K$ -shell) conditions was observed. This effect is not intrinsic to the technology, but rather is a feature of the ECS combined with the particulars of this experiment. During calibration with the  $^{133}\text{Ba}$  source, the incident power was  $\sim 50$  keV/sec/pixel versus under 3 keV/sec/pixel from xenon  $K$ -shell emission from SuperEBIT. By placing filters in front of the  $^{133}\text{Ba}$  source, we were able to measure the x-ray calorimeter's response as a function of incident power, and thus correct for this shift. The shift in the Cs  $K\alpha$  lines as a function of incident power is shown in Fig. 2.

For power levels under 9 keV/sec/pixel, the shift in the Cs  $K\alpha$  lines is about 8 eV compared to the power level at which daily calibration were performed. Since xenon  $K$ -shell data were recorded at powers under 3 keV/sec/pixel, the average value of the power shift for powers under 9 keV/sec/pixel,  $8.12 \pm 0.76$  eV, was used to correct for the discrepancy in incident power between calibration data and xenon  $K$ -shell data.

The positions of the xenon lines were determined by applying Gaussian fit functions to the spectrum shown in Fig. 1. Table I lists the results for the measured transition energies for the hydrogenlike system. The data are compared to the calculations by Johnson and Soff [20] and show excellent agreement with theory. The hydrogenlike transitions Lyman- $\alpha_2$  and Lyman- $\alpha_3$  are not spectroscopically resolved. This allows for a test of theoretical predictions of the intensity of the magnetic dipole ( $M1$ ) transition. In lower- $Z$  ions, the  $2s_{1/2}$  excited state is almost purely deexcited though a two-photon transition to the

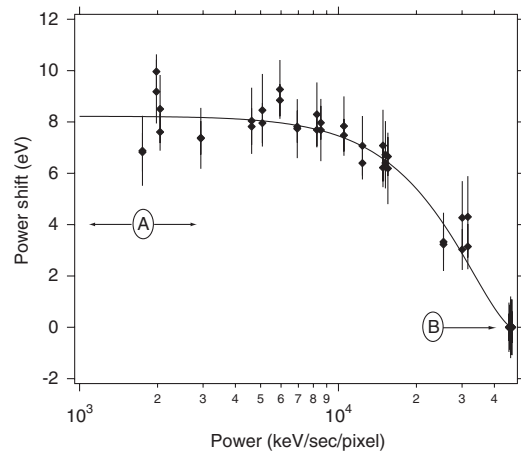


FIG. 2. The power shift of the Cs  $K\alpha$  calibration lines as a function of incident power. Xenon  $K$ -shell data were taken at a power of under 3 keV/sec/pixel, denoted by region A. Daily calibrations with  $^{133}\text{Ba}$  were performed at a power level of 50 keV/sec/pixel, denoted by B and are used to provide the reference value for the power shift. The solid line is a cubic fit to the data, which is approximately linear as the values of the nonlinear terms are several orders of magnitude smaller. The error bars shown here are statistical.

TABLE I. Experimental and theoretical  $K$ -shell transition energies for hydrogenlike xenon.

Label	Transition	Energy (eV)	
		Measurement	Theory <sup>a</sup>
Lyman- $\alpha_1$	$(2p_{3/2})_{3/2} \rightarrow (1s_{1/2})_{1/2}$	$31\,284.9 \pm 1.8$	31 283.77
Lyman- $\alpha_3$	$(2s_{1/2})_{1/2} \rightarrow (1s_{1/2})_{1/2}$		30 863.49
Lyman- $\alpha_2$	$(2p_{1/2})_{1/2} \rightarrow (1s_{1/2})_{1/2}$		30 856.36
Blend <sup>b</sup>		$30\,859.3 \pm 2.0$	30 857.73 <sup>c</sup>

<sup>a</sup>Johnson and Soff .<sup>b</sup>Blend of Lyman- $\alpha_3$  and Lyman- $\alpha_2$ .<sup>c</sup>Predicted value using line intensities as calculated from FAC [21] and using transition energy values of Johnson and Soff [20].

ground state, while in high- $Z$  ions the two-photon deexcitation is reduced in favor of a  $M1$  transition. Using the ratio of the line intensity of Lyman- $\alpha_2$  to Lyman- $\alpha_3$  transitions (1:4.18) at an electron beam energy of 114 keV calculated from the flexible atomic code [21] and the transition energies taken from Johnson and Soff [20], we find that the predicted line centroid of the Lyman- $\alpha_2$ , Lyman- $\alpha_3$  blend should be at 30 857.73 eV. This value is consistent with our experimental value of  $30\,859.3 \pm 2.0$  eV.

The uncertainty in the determination of the hydrogenlike lines is the quadrature sum of the power shift uncertainty of 0.76 eV, the statistical error of 1.45 eV for Lyman- $\alpha_1$  and 1.74 eV for the Lyman- $\alpha_{2,3}$  line, the uncertainty in the energy scale of 0.6 eV, and the 0.15 eV uncertainty in the determination of the Cs  $K\alpha$  lines used for calibration.

Table II lists the experimentally determined transition energies for heliumlike xenon ions compared to the calculations by Drake [26], Plante *et al.* [25], Chen *et al.* [23], Cheng *et al.* [22], and Artemyev *et al.* [24]. Drake uses a nonrelativistic approach to solve for the wave functions, and an approximate solution to the QED shifts based on one-electron QED. The other calculations use all-order relativistic configuration interaction methods taken from the no-pair Hamiltonian [27], and differ from each other in the way in which they treat the QED corrections. Plante *et al.* and Chen *et al.* (only for lines  $x$  and  $z$ ) use the approach of Drake for the QED shifts, whereas Cheng *et al.* (only for lines  $w$  and  $y$ ) use an *ab initio* approach

to solve for the QED shifts to first order in QED. Artemyev *et al.* use an *ab initio* approach to second order in QED.

The uncertainty in the measurement of the singlet line,  $w$ , of 1.2 eV, is found by adding in quadrature the power shift uncertainty, the statistical uncertainty of 0.67 eV, the uncertainty in the determination of the energy scale, and the uncertainty in the determination of the Cs  $K\alpha$  lines used for calibration. The uncertainties in the measurement of the triplet lines,  $x$ ,  $y$ , and  $z$ , are found by adding the power shift uncertainty, the statistical error of 0.85 eV, 1.01 eV, and 0.76 eV (for line  $y$ , line  $x$ , and line  $z$ , respectively), the energy scale uncertainty, the uncertainty from unresolved line blends from the lithiumlike charge state [28] of 0.5 eV, 0.85 eV, and 0.3 eV (for line  $y$ , line  $x$ , and line  $z$ , respectively) in quadrature.

As a metric to compare each theory with experiment the absolute average deviation from experiment for each theory was computed. It is found that the calculations by Cheng *et al.* [22] and Artemyev *et al.* [24] have the smallest average differences from experiment of 0.38 eV and 0.665 eV, respectively. For the calculations of Chen *et al.* [23], Plante *et al.* [25], and Drake [26] the average deviation from experiment is 0.825, 0.875, and 1.15 eV, respectively. While these differences are generally smaller than our measurement's uncertainty and would require yet another order of magnitude improvement in precision, they do favor the more complete calculations of Cheng *et al.* and Artemyev *et al.* As can be seen from Table II two of

TABLE II. Experimental and theoretical  $K$ -shell transition energies of heliumlike xenon.

Label	Transition	Energy (eV)				
		Measurement	a	b	Theory	
			c	d		
$w$	$(1s2p_{3/2})_1 \rightarrow (1s^2)_0$	$30\,631.2 \pm 1.2$	30 630.64	30 630.05	30 629.68	30 629.28
$x$	$(1s2p_{3/2})_2 \rightarrow (1s^2)_0$	$30\,594.5 \pm 1.7$	30 594.96	30 594.36	30 593.93	30 593.54
$y$	$(1s2p_{1/2})_1 \rightarrow (1s^2)_0$	$30\,207.1 \pm 1.4$	30 206.90	30 206.27	30 205.87	30 205.58
$z$	$(1s2s_{1/2})_1 \rightarrow (1s^2)_0$	$30\,128.6 \pm 1.3$	30 129.79	30 129.14	30 128.78	30 128.40

<sup>a</sup>Cheng *et al.* [22] for lines  $y$  and  $w$  and Chen *et al.* [23] for lines  $z$  and  $x$ .<sup>b</sup>Artemyev *et al.* [24].<sup>c</sup>Plante *et al.* [25].<sup>d</sup>Drake [26].

Drake's values and one of Plante *et al.*'s values fall outside of our  $1\sigma$  error bar.

Previous measurements carried out with solid state detectors either neglected the blend of line  $w$  with the triplet line  $x$ , or mentioned that the measured feature is the combination of the two and thus cannot accurately test theory [6,9]. The present measurement is the first to account for the blend in this high atomic number element.

In summary, we find that for the two calculations that include *ab initio* QED contributions, the average deviation from experiment is smallest. Furthermore, when looking at line  $w$ , which has the smallest error bar, the same two calculations are the only ones that fall within the experimental error. Thus, our measurement technique is able to select calculations based on how QED contributions are calculated and is en route to obtaining a 1 eV measurement in the  $K$ -shell transition energy in highly charged uranium ions.

We gratefully acknowledge fruitful discussions with Mau Chen, as well as expert technical support on EBIT by Ed Magee, and thank John Gyax and Jonathan King for help in building and designing the ECS spectrometer. This work was performed under the auspices of the U.S. Department of Energy by Lawrence Livermore National Laboratory under Contract No. DE-AC52-07NA27344 and supported by NASA Astronomy and Physics Research and Analysis Program (APRA) grants to LLNL and NASA/GSFC.

---

\*Present address: Extreme Matter Institute, Darmstadt, Germany.

dbthorn@gsi.de

- [1] A. Schäfer, G. Soff, and P. Indelicato, *Phys. Rev. A* **40**, 7362 (1989).
- [2] M. S. Pindzola, *Phys. Rev. A* **47**, 4856 (1993).
- [3] L. N. Labzowsky, A. V. Nefiodov, G. Plunien, G. Soff, R. Marrus, and D. Liesen, *Phys. Rev. A* **63**, 054105 (2001).
- [4] K. Widmann, P. Beiersdorfer, V. Decaux, and M. Bitter, *Phys. Rev. A* **53**, 2200 (1996).
- [5] C. T. Munger and H. Gould, *Phys. Rev. Lett.* **57**, 2927 (1986).
- [6] J. P. Briand, P. Chevallier, P. Indelicato, K. P. Ziock, and D. Dietrich, *Phys. Rev. Lett.* **65**, 2761 (1990).
- [7] T. Stöhlker *et al.*, *Phys. Rev. Lett.* **85**, 3109 (2000).
- [8] T. Stöhlker *et al.*, *Phys. Rev. Lett.* **71**, 2184 (1993).
- [9] J. P. Briand, P. Indelicato, A. Simionovici, V. S. Vicente, D. Liesen, and D. Dietrich, *Europhys. Lett.* **9**, 225 (1989).
- [10] A. Gumberidze *et al.*, *Phys. Rev. Lett.* **94**, 223001 (2005).
- [11] C. K. Stahle, D. McCammon, and K. D. Irwin, *Phys. Today* **52**, No. 8, 32 (1999).
- [12] D. McCammon *et al.*, *J. Low Temp. Phys.* **151**, 715 (2008).
- [13] P. Beiersdorfer *et al.*, *Science* **300**, 1558 (2003).
- [14] E. Silver *et al.*, *Nucl. Instrum. Methods Phys. Res., Sect. A* **444**, 156 (2000).
- [15] R. L. Kelley *et al.*, *Astron. Soc. Jpn.* **59**, 77 (2007).
- [16] H. Bruhns, J. Braun, K. KubiCek, J. R. C. Lopez-Urrutia, and J. Ullrich, *Phys. Rev. Lett.* **99**, 113001 (2007).
- [17] D. B. Thorn, G. V. Brown, J. H. T. Clementson, H. Chen, M. Chen, P. Beiersdorfer, K. R. Boyce, C. A. Kilbourne, F. S. Porter, and R. L. Kelley, *Can. J. Phys.* **86**, 241 (2008).
- [18] F. S. Porter *et al.*, *Can. J. Phys.* **86**, 231 (2008).
- [19] D. A. Knapp, R. E. Marrs, S. R. Elliot, E. W. Magee, and R. Zasadzinski, *Nucl. Instrum. Methods Phys. Res., Sect. A* **334**, 305 (1993).
- [20] W. R. Johnson and G. Soff, *At. Data Nucl. Data Tables* **33**, 405 (1985).
- [21] M. F. Gu, *Can. J. Phys.* **86**, 675 (2008).
- [22] K. T. Cheng, M. H. Chen, W. R. Johnson, and J. Sapirstein, *Phys. Rev. A* **50**, 247 (1994).
- [23] M. H. Chen, K. T. Cheng, and W. R. Johnson, *Phys. Rev. A* **47**, 3692 (1993).
- [24] A. N. Artemyev, V. M. Shabaev, V. A. Yerokhin, G. Plunien, and G. Soff, *Phys. Rev. A* **71**, 062104 (2005).
- [25] D. R. Plante, W. R. Johnson, and J. Sapirstein, *Phys. Rev. A* **49**, 3519 (1994).
- [26] G. W. F. Drake, *Can. J. Phys.* **66**, 586 (1988).
- [27] J. Sapirstein, *Phys. Scr.* **36**, 801 (1987).
- [28] The intensities of the lithiumlike transitions that blend with the heliumlike transitions were made by relating the calculated intensities of the blended lines with the known intensity of the lithiumlike resonance transition  $q$  (see Fig. 1). The largest contamination of a lithiumlike line is estimated as no greater than 3% and that is for contamination of line  $x$ .
- [29] A. H. Gabriel, *Mon. Not. R. Astron. Soc.* **160**, 99 (1972).
- [30] M. Bitter, K. W. Hill, N. R. Sauthoff, P. C. Eftimion, E. Meservey, W. Roney, S. von Goeler, R. Horton, M. Goldman, and W. Stodieck, *Phys. Rev. Lett.* **43**, 129 (1979).
- [31] P. Beiersdorfer, T. Phillips, V. L. Jacobs, K. W. Hill, M. Bitter, S. von Goeler, and S. M. Kahn, *Astrophys. J.* **409**, 846 (1993).